J. Phys. B: At. Mol. Opt. Phys. 28 (1995) 487–504. Printed in the UK

Electron collisions with NO: elastic scattering and rovibrational ($0 \rightarrow 1, 2, 3, 4$) excitation cross sections

B Mojarrabi†, R J Gulley‡, A G Middleton†, D C Cartwright§, P J O Teubner†, S J Buckman‡ and M J Brunger†

† Institute for Atomic Studies, Flinders University of South Australia, GPO Box 2100, Adelaide, SA 5001, Australia

‡ Electron Physics Group, Research School of Physical Sciences and Engineering, Australian National University, Canberra, ACT 0200, Australia

§ Theoretical Division, Los Alamos National Laboratories, Los Alamos, NM, USA

Received 11 October 1994

Abstract. The relative flow technique, utilizing helium as a cross section standard, has been applied to measure absolute elastic differential cross sections for electron scattering from nitric oxide (NO). The present elastic measurements were conducted at nine energies in the range 1.5–40 eV, which represents an important extension to the only previous study of this system by Kubo and co-workers. Furthermore, the uncertainties in the present data are significantly reduced in comparison to those quoted in the earlier work. The current elastic differential cross sections were measured at the Australian National University over an angular range 10°–130°. We also report the first measurements of absolute differential cross sections for rovibrational ($0 \rightarrow 1, 2, 3, 4$) excitation of the NO ground electronic state. These were conducted at six energies in the range 7.5–40 eV and were measured at Flinders University over the angular range 10°–90°. The differential cross sections for both the elastic and inelastic processes are compared with the results of the recent Born-closure Schwinger variational method calculation of Mu-Tao Lee and colleagues.

1. Introduction

There has been renewed interest in nitric oxide (NO) as a scattering system since its important role in the catalytic destruction of ozone in the stratosphere was confirmed (Mason and Newell 1989, Kirby 1993). From a more fundamental perspective electron scattering by NO represents a considerable challenge to theorists in that it is an open-shell molecule and it possesses a small, but significant, permanent dipole moment of 0.157 D. In the former case, particularly at low energies, Tennyson and Noble (1986) have shown that for elastic scattering by open-shell molecules, polarization effects are particularly important because of the presence of low-lying electronically excited states. In the latter case, the very forward angle behaviour of the elastic differential cross section (DCS) is expected to be divergent (Norcross and Collins 1982) within a fixed-nuclei treatment. This effect can only be treated by the inclusion of nuclear motion in the Hamiltonian.

The pioneering experimental study of electron scattering from NO was undertaken by Brüche (1927) who used a Ramsauer technique to measure the absolute total cross section in the energy range 1–49 eV. Subsequently very little work has been done on absolute cross section determinations for electron–NO scattering, with most of the experimental studies having concentrated on the ionization process (Hagstrum and Tate 1941, Clautier and Schiff 1959, Rapp and Englander-Golden 1965, Rapp and Briglia 1965, Hierl and Franklin 1967,

0953-4075/95/030487+18$19.50

Kadota and Kaneko 1977) and on dissociative electron attachment (Frost and McDowell 1958, Dorman 1966, van Brunt and Kieffer 1974, Mazeau *et al* 1978, Krishnakumar and Srivastava 1988). For completeness we also note the coincidence (e,2e) studies of Fantoni *et al* (1982) and Brion *et al* (1982) who measured momentum distributions of the various valence states to investigate the quality of the quantum chemical basis sets of states then available in the literature for NO. The results of both these studies were inconclusive because the energy resolution of both studies was marginal.

Strong resonance effects in electron–NO scattering have been observed in low-energy transmission functions by Boness and Hasted (1966), Ehrhardt and Willmann (1967), Boness *et al* (1968), Hasted and Awan (1969), Zecca *et al* (1974), Szmytkowski and Maciag (1991) and in the backscattered current by Burrow (1974). More detailed experimental studies of the resonant scattering below 3 eV were performed by Spence and Schulz (1971) and Tronc *et al* (1975) with the observed oscillatory structure being attributed to vibrational series of NO^- shape resonances. In particular these short-lived negative ions were found to belong to a three-member multiplet of $^3\Sigma^-$, $^1\Delta$ and $^1\Sigma^+$ symmetries (Tronc *et al* 1975). Using a simple formalism, Teillet-Billy and Fiquet-Fayard (1977) analysed these resonant structures and estimated the spectroscopic constants of the two lowest resonances. The resonance positions and widths calculated by Tennyson and Noble (1986), using an *R*-matrix formalism, were found to be in quite good agreement with the measurements of Tronc *et al* (1975). For completeness, we also note the calculation of Koike (1975) on low-energy resonances in NO. Further resonance effects at impact energies up to about 20 eV were observed in transmission spectroscopy by Sanche and Schulz (1972) and in the high-resolution experiments by Gresteau *et al* (1977, 1979a, b). These latter experiments obtained significant results on the decay of Feshbach resonances in NO. More recently, Tronc *et al* (1980), King *et al* (1980) and Camilloni *et al* (1987) have studied the inner-shell excited states of NO. Experiments on the radiative electron impact excitation of NO (Stone and Zipf 1972, Povch *et al* 1972, Imami and Borst 1975, van Sprang *et al* 1979 and Skubenich *et al* 1977) were partly stimulated by the role of NO in auroral displays.

Aside from the experimental studies of Brüche (1927) and Szmytkowski and Maciag (1991), the only other absolute cross sections reported in the literature are due to Dalba *et al* (1980) and Kubo *et al* (1981). Dalba *et al* performed a Ramsauer-type experiment to report total scattering cross sections in the energy range 121–1444 eV, whilst Kubo *et al* employed a version of the relative flow technique, with the elastic helium cross sections of Register *et al* (1980) as the cross section standard, to measure absolute elastic DCSs at the energies 5, 10, 15, 20, 25 and 30 eV and over the angular range 30°–140°, in 10° increments. The uncertainty on these data was quoted at ±30%. From a theoretical perspective the situation is even worse with only the quite recent Born-closure Schwinger variational method (BCSVM) calculation of Mu-Tao Lee *et al* (1992), the optical model approach of Jain *et al* (1993) and the Schwinger multichannel method (SMC) of da Paixao *et al* (1993) being available in the literature. The study of Mu-Tao Lee *et al* reported DCSs for elastic scattering at selected energies in the range 5–500 eV. Where possible, comparison was made with the data of Kubo *et al*, the level of agreement between theory and experiment was fair at 10 and 20 eV and quite poor at 5 eV, with the BCSVM calculation overestimating the DCS by about a factor of 2. Mu-Tao Lee *et al* noted that this discrepancy at 5 eV could be due to the neglect of polarization effects in their study which, as previously pointed out by Tennyson and Noble (1986), become important for low-energy elastic scattering by open-shell molecules. In fact, even at 10 and 20 eV the data of Kubo *et al*, with uncertainties of ±30%, do not really provide a stringent test of the BCSVM calculation. More recently Mu-Tao Lee (1994) has extended the BCSVM model to allow for nuclear motion, thereby enabling calculations of

rovibrational DCSs ($v = 0 \rightarrow 1, 2$) at certain energies in the range 5–30 eV. The calculation by Jain *et al*, based on the work of Gianturco and Jain (1986), employs an optical potential approach where the interaction potential consists of the static, polarization and exchange terms. Results are presented at 5, 10 and 20 eV and were generally found to be in quite marginal agreement with the experimental results of Kubo *et al* (1981). The SMC calculation of da Paixao *et al* reported only a single result at 10 eV and agreement with Kubo *et al* seemed fair, except at forward angles. However, as we do not have tables of the data for either Jain *et al* or da Paixao *et al* we do not discuss their results further at this time.

In this paper we extend the scope of the measurements of Kubo *et al* by reporting absolute elastic DCS data at the energies 1.5, 3, 5, 7.5, 10, 15, 20, 30 and 40 eV and also by taking great care to minimize possible sources of uncertainty such that the error is typically between 6–12%. We also report the first measurements of absolute rovibrational DCSs ($v = 0 \rightarrow 1, 2, 3, 4$) at the energies 7.5, 10, 15, 20, 30 and 40 eV. Both data sets provide new experimental results against which the recent calculations of Mu-Tao Lee and co-workers (1992, 1994) can be critically compared and judged.

This paper is the result of a joint Flinders University, Australian National University (ANU) and Los Alamos collaborative effort and is the first in a series of papers that will look at electron impact phenomena in NO. In the next section we briefly discuss both the Flinders University and the ANU crossed beam experiments with which the present rovibrational and elastic DCSs were made. The relevant techniques employed in these measurements are also discussed in this section. Section 3 sees us present and discuss both our differential and integral elastic cross sections and our rovibrational differential and integral cross sections. In both these sections, comparison with available theory and other experiments is made. The paper is completed with some conclusions being drawn in section 4.

2. Experimental considerations

The present experiments were carried out in two separate laboratories at Flinders University and the Australian National University using two different crossed electron–molecular beam spectrometers. Both of these devices, and the techniques used to operate them, have been described in detail previously (e.g. Brunger and Teubner 1990, Gulley *et al* 1994 respectively) so we will only give a brief discussion of relevant details here. Both spectrometers use electrostatic hemispherical monochromators and electron optics for the production of energy resolved electron beams from thoriated tungsten sources. Whilst there are some differences in the design of the energy selectors and optics, both produce electron beams which, in this case, have energy widths of around 40–60 meV (FWHM) and beam currents of 1–5 nA. Energy calibration in each case was achieved either by reference to the energy of the He^- $1s2s^2$ ^2S resonance at 19.367 eV or the position of the low-lying shape resonance peaks in elastic scattering from N_2 (Rohr 1977). An electron energy loss spectrum obtained on the Flinders apparatus at an incident energy of 15 eV and a scattering angle of 50° is shown in figure 1. This spectrum clearly shows that the vibrational quanta are resolved from one another and the elastic peak.

The Flinders apparatus has been used for measurements of elastic scattering and vibrational excitation angular distributions over the energy range from 7.5–40 eV and an angular range from 10–90°. In these measurements careful consideration has been given to the optimization of the transmission of the post-collision electron optics (Middleton *et al* 1994) to enable accurate determinations of the ratios of the vibrational excitation intensities to that for elastic scattering. The maximum energy difference for the outgoing electrons

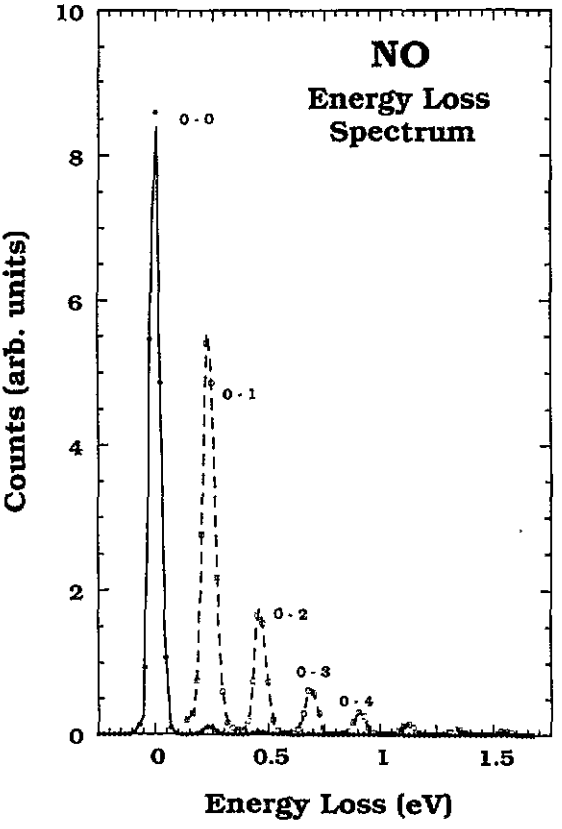

Figure 1. Energy loss spectrum for NO at an incident energy of 15 eV and a scattering angle of 50°. The present data (●) and the present inelastic data scaled by a factor of 50 (□) are shown.

is around 0.9 eV (the energy difference between elastic scattering and $v = 0$–4 vibrational excitation) and at an incident energy of 7.5 eV, the lowest energy at which the present vibrational excitation studies were carried out, this represents a change of about 12% in the scattered electron energy. The angular efficiency of the apparatus for a particular set of electron optical voltages and gas driving pressures is determined by measurements of angular distributions for elastic scattering from helium at each energy. In this way, by comparison with standard helium cross sections (Nesbet 1979) at each energy, an angular correction factor can, if necessary, be determined. The measurements carried out on this apparatus are not absolute, but can be placed on an absolute scale by normalization to appropriate experiment or theory for any of the excitation channels concerned.

We note that the lowest reported energy of the present rovibrational excitation study was 7.5 eV. An attempt to extend our measurements to 5 eV was made but the $0 \rightarrow 1$ cross section was found to be prohibitively small there. Similarly at 3 eV, on the basis of our integral elastic data and the grand total cross section of Szmytkowski and Maciag (1991), we would also anticipate that the $0 \rightarrow 1$ cross section would be very small.

The ANU apparatus has been designed specifically for absolute low-energy electron scattering measurements. In the present work it has been used to study absolute elastic scattering cross sections at energies between 1.5 and 40 eV and over an angular range from 10 to 130°. In particular measurements have been conducted at identical energies to that from the Flinders apparatus in order to provide a mechanism for normalizing both the elastic and rovibrational measurements from the Flinders experiments. The ANU measurements are placed on an absolute scale by use of the relative flow technique (see for example

Srivastava *et al* 1975, Nickel *et al* 1989, Buckman *et al* 1993). By measuring ratios of scattered intensities for NO and He at each scattering angle under carefully controlled conditions (Buckman *et al* 1993), the technique yields elastic scattering cross sections for NO with uncertainties between 6 and 12%. Of particular utility in the present study, given the highly reactive nature of NO with hot filament sources, was the ability to be able to conduct measurements of scattering ratios with both gases present in the apparatus.

The absolute uncertainty on the elastic scattering cross sections measured with the ANU spectrometer represents a combination of statistical and systematic uncertainties including those associated with the relative flow rate measurements and estimates of the effects of small fluctuations in gas pressure and electron beam current. The Flinders data, for both elastic scattering and vibrational excitation, have been placed on an absolute scale by normalizing to the ANU elastic cross section, typically at a scattering angle of 60°. As a result, the uncertainties on the Flinders cross sections are typically between 10–14% for the elastic channel. This gives an error between 15 and 27% for the vibrational excitation results.

3. Results and discussion

3.1. Elastic scattering

Absolute DCSs for elastic electron scattering from NO are presented in table 1 and shown, at selected energies, in figures 2 and 3, where they are also compared to the only other available experiment and theory.

Table 1. Absolute elastic and rovibrational ($0 \rightarrow 1, 2$) integral cross sections (10^{-16} cm^2) for electron scattering from nitric oxide. Figures in brackets indicate the absolute uncertainty expressed as a percentage.

E_0 (eV)	Q_{el}	$Q_{0\rightarrow1}$	$Q_{0\rightarrow2}$	Q_t
1.5	8.750 (30)	—	—	8.750 (30)
3.0	8.385 (30)	—	—	8.385 (30)
5.0	8.087 (20)	—	—	8.087 (20)
7.5	7.676 (20)	0.028 (25)	—	7.704 (20)
10.0	7.499 (20)	0.074 (20)	0.014 (30)	7.587 (20.1)
15.0	7.678 (20)	0.270 (25)	0.073 (30)	8.021 (20.1)
20.0	7.087 (20)	0.097 (25)	0.022 (30)	7.206 (20.1)
30.0	6.920 (20)	0.022 (25)	—	6.942 (20)
40.0	5.374 (30)	0.014 (35)	—	5.388 (30)

The cross sections for energies below 10 eV are shown in figure 2. The most surprising and unusual aspect of the cross sections at these energies is the forward angle behaviour. At 1.5 eV (figure 2(*a*)), the DCS exhibits a clear maximum at around 60°, dropping off in magnitude towards both forward and backward scattering angles. This behaviour is even more marked at an incident energy of 3 eV (figure 2(*b*)) where the cross section drops rapidly from its maximum value of about 1.1×10^{-16} cm^2 sr^{-1} at around 50–60°. Unfortunately there are no other experimental or theoretical results with which to compare at either of these energies. At 5 eV (figure 2(*c*)) the decrease in the cross section in the forward direction is once again evident, but not so pronounced, and the cross section maximum of around 1.2×10^{-16} cm^2 sr^{-1} has again shifted to a lower angle, in this case about 40–50°.

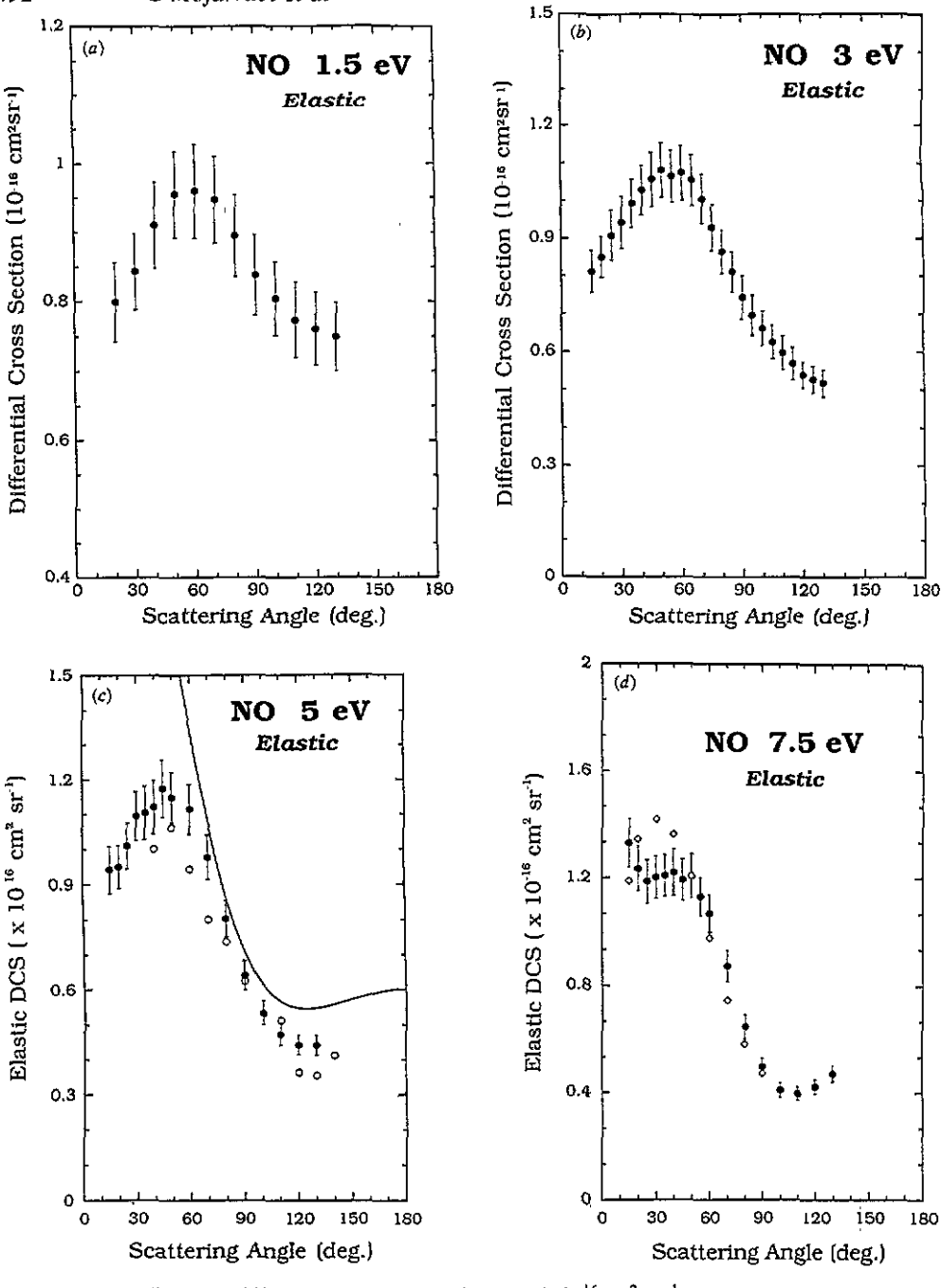

Figure 2. Differential cross sections, in units of 10^{-16} cm^2 sr^{-1}, for elastic scattering from NO at (*a*) 1.5 eV, (*b*) 3 eV, (*c*) 5 eV and (*d*) 7.5 eV. The present data from ANU (●) and Flinders (◇), are compared against the earlier results of Kubo *et al* (○) and the BCSVM calculation of Mu-Tao Lee *et al* (——).

Here there are both other experimental and theoretical results available for comparison. The experimental cross section of Kubo *et al* (1981) is in good general agreement with the present results, exhibiting the same overall shape with a maximum at around 50° and

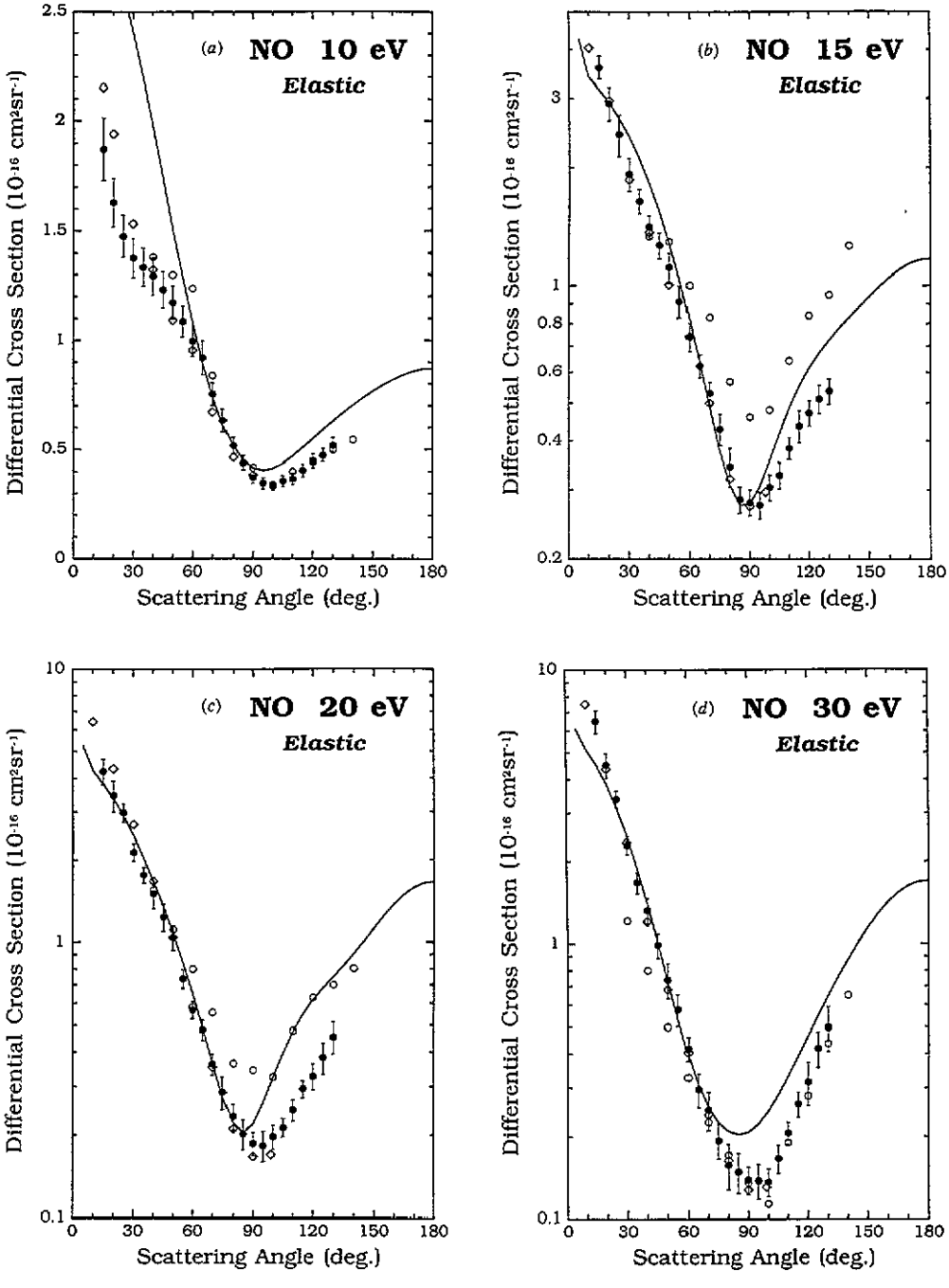

Figure 3. Differential cross sections, in units of 10^{-16} cm^2 sr^{-1}, for elastic scattering from NO at (*a*) 10 eV, (*b*) 15 eV, (*c*) 20 eV and (*d*) 30 eV. The present data from ANU (●) and Flinders (◇), are compared against the earlier results of Kubo *et al* (○) and the BCSVM calculation of Mu-Tao Lee *et al* (——).

a minimum at 130°, although there are some small differences in absolute magnitude over this range. The theoretical curve of Mu-Tao Lee *et al*, whilst exhibiting similarities to

the experimental results at scattering angles above about 60°, is substantially larger than the experiment at small angles and, although the axis of the graph has been truncated, the theoretical cross section does exhibit a local maximum at small angles. Finally at 7.5 eV (figure 2(*d*)), we can compare the present Flinders and ANU data. We believe the level of agreement between them is good over the entire common angular range, within the combined uncertainties on the respective data sets (≈ 11% on the Flinders Data). Both cross sections exhibited the same angular behaviour we saw previously at forward angles for lower energies (figures 2(*a*)–(*c*)), although the current ANU measurement perhaps suggests a rather flatter shoulder between 20–50° than seen at the lower energies.

This behaviour at forward angles, where the cross section decreases as a function of angle over a range of fairly low energies, is not unique to the elastic cross section for NO but has been observed by us, and in other laboratories, in a range of other diatomic molecules. We have observed similar DCS structure in both N_2 (Sun *et al* 1994) and O_2 (Sullivan *et al* 1994) and it has also been observed in CO (Tanaka *et al* 1978). We can only speculate upon the reason for this behaviour but it appears to be associated with long-range interactions which are mediated, principally, by the polarization potential. We note that these molecules all have similar static dipole polarizabilities and as a result one might naively expect similar trends in the forward angle scattering behaviour. Indeed we have found that in N_2 (Sun *et al* 1994) very large numbers of partial waves were required to both ensure convergence of the DCS calculations at forward angles and to show the measured decrease in the cross section at forward angles.

At higher energies the trends in the shape of the DCS, shown at low energies, continue to develop, with the scattering becoming more enhanced in the forward direction and the cross section minimum becoming deeper and moving to lower angles. At 10 eV (figure 3(*a*)) the present data, from both Flinders and ANU, are compared with the data of Kubo *et al*. The agreement, particularly in the shape of the two present measurements, is quite good, as is the overall agreement with Kubo *et al*. The theoretical calculation reproduces the gross features of the cross section but not the detailed structure, particularly the shoulder at forward angles. At 15 eV (figure 3(*b*)) the agreement between the two present data sets is excellent and both are uniformly lower and different in shape from the DCS of Kubo *et al*. The theory is in considerably better agreement with the present results at this energy. At 20 eV (figure 3(*c*)) we see a similar result, excellent agreement between the present results which are again lower than those of Kubo *et al*, particularly at large scattering angles. Finally at 30 eV (figure 3(*d*)) the present results are again in excellent agreement over the entire, common angular range and at angles greater than about 70° they are also in excellent agreement with Kubo *et al* but lower in magnitude than the theory. At smaller scattering angles the present results lie above those of Kubo *et al* but are in good agreement with the theory. At 40 eV (not shown) the two present sets of data are once again in excellent agreement.

The present elastic DCSs have been extrapolated to 0 and 180° and integrated to yield both total elastic cross sections and elastic momentum transfer cross sections. The extrapolation to forward and backward angles was largely done by eye although in those cases where there was theory available for comparison, the shape of the theory has been considered when making the otherwise, somewhat subjective, extrapolation. The cross sections arising from this procedure are tabulated in tables 1 and 2 and the elastic momentum transfer cross section is plotted in figure 4. The total elastic data are discussed in the next section.

The momentum transfer cross section, as shown in figure 4, is compared once again with the theory of Mu-Tao Lee *et al* (1992). The present cross section, which demonstrates

Table 2. Absolute elastic momentum transfer cross sections (10^{-16} cm^2) for electron scattering from nitric oxide. Figures in brackets indicate the absolute uncertainty expressed as a percentage.

E_0 (eV)	$Q_{mt}^{elastic}$
1.5	7.030 (30)
3.0	6.152 (30)
5.0	5.513 (20)
7.5	4.880 (20)
10.0	4.496 (20)
15.0	4.044 (20)
20.0	3.089 (20)
30.0	2.635 (20)
40.0	1.666 (30)

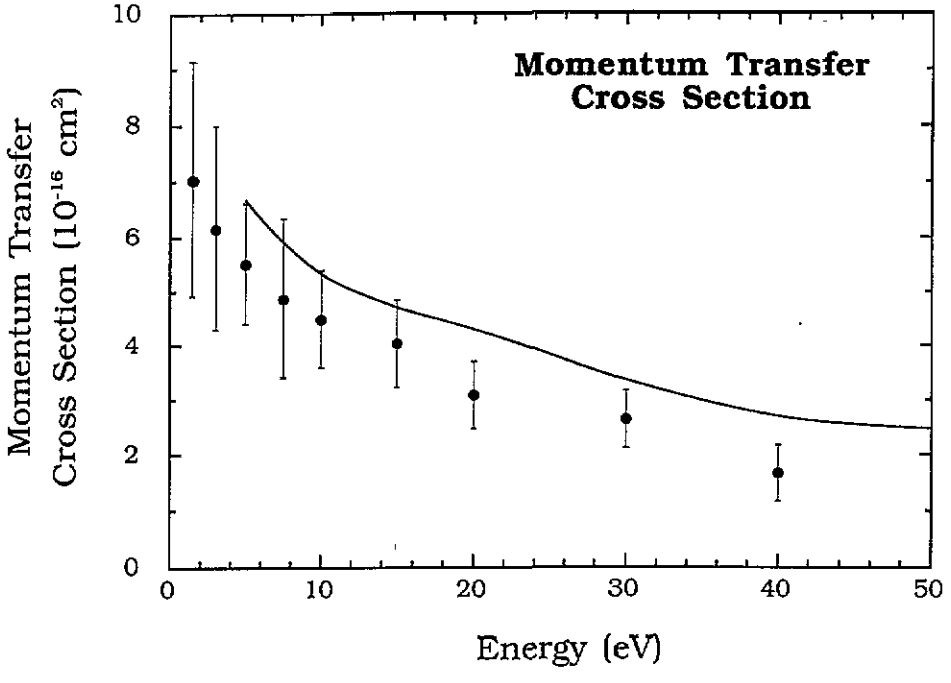

Figure 4. Elastic momentum transfer cross sections, in units of 10^{-16} cm^2, for electron scattering from NO. The present results (●) are compared against the BCSVM calculation of Mu-Tao Lee *et al* (——).

a gradual decrease in magnitude from 1 to 40 eV, is uniformly lower than the theory, as might be expected from the previous comparisons at the DCS level.

3.2. Rovibrational excitation

DCSs for electron impact excitation of the $0 \rightarrow 1$, $0 \rightarrow 2$, $0 \rightarrow 3$ and $0 \rightarrow 4$ vibrationally inelastic transitions of the NO ground molecular state are given in tables 3–7, respectively. Representative examples of these data and the results of the BCSVM calculation of Mu-Tao Lee (1994) will be illustrated in figures 6–10. The errors in the present rovibrational data represent plus or minus one standard deviation and are typically in the range 15–19% for the $v = 0 \rightarrow 1$ transition, 16–20% for the $v = 0 \rightarrow 2$ transition, 20–23% for the $v = 0 \rightarrow 3$

Table 3. Absolute elastic DCSs (10^{-16} cm^2 sr^{-1}) for electron scattering from nitric oxide. Figures in brackets indicate the absolute uncertainty expressed as a percentage.

	E_0 (eV)								
θ_e	1.5	3.0	5.0	7.5	10.0	15.0	20.0	30.0	40.0
10	—	—	—	—	—	—	—	—	9.874 (7.5)
15	—	0.812 (6.9)	0.941 (7.1)	1.330 (6.7)	1.870 (7.6)	3.600 (6.9)	4.236 (11.1)	6.484 (10.4)	6.594 (7.4)
20	0.799 (7.1)	0.850 (6.5)	0.949 (6.5)	1.234 (6.7)	1.629 (6.7)	2.907 (9.7)	3.444 (13.6)	4.490 (10.9)	4.364 (7.3)
25	—	0.908 (7.4)	1.010 (6.4)	1.186 (6.8)	1.475 (6.4)	2.424 (12.1)	2.968 (8.7)	3.387 (8.0)	3.042 (7.3)
30	0.843 (6.6)	0.942 (7.3)	1.095 (6.4)	1.202 (6.6)	1.375 (6.4)	1.922 (9.6)	2.132 (8.0)	2.290 (8.5)	1.958 (7.3)
35	—	0.993 (6.5)	1.104 (6.9)	1.209 (6.4)	1.333 (6.5)	1.639 (7.2)	1.764 (7.4)	1.671 (9.6)	1.275 (7.3)
40	0.910 (6.8)	1.028 (6.4)	1.121 (6.9)	1.221 (7.1)	1.292 (6.5)	1.409 (6.7)	1.502 (12.5)	1.323 (11.1)	0.885 (7.4)
45	—	1.056 (6.8)	1.174 (7.1)	1.193 (6.5)	1.230 (6.8)	1.264 (7.6)	1.231 (12.0)	0.987 (10.7)	0.578 (8.3)
50	0.955 (6.6)	1.081 (6.6)	1.148 (6.4)	1.207 (6.8)	1.172 (6.5)	1.109 (8.6)	1.036 (10.8)	0.739 (15.2)	0.410 (8.0)
55	—	1.064 (6.6)	—	1.130 (6.5)	1.086 (6.4)	0.910 (9.3)	0.737 (8.5)	0.576 (13.7)	0.318 (8.2)
60	0.960 (7.1)	1.074 (6.8)	1.114 (6.5)	1.067 (6.6)	0.996 (7.1)	0.739 (8.4)	0.567 (8.0)	0.417 (11.0)	0.245 (7.5)
65	—	1.054 (6.4)	—	—	0.920 (8.5)	0.622 (6.7)	0.481 (9.2)	0.296 (14.6)	0.189 (7.8)
70	0.947 (6.7)	1.004 (6.6)	0.976 (6.4)	0.873 (6.7)	0.752 (6.9)	0.529 (6.4)	0.361 (9.4)	0.249 (15.9)	0.149 (8.0)
75	—	0.928 (6.6)	—	—	0.631 (8.3)	0.428 (9.1)	0.285 (14.1)	0.193 (15.1)	0.121 (8.7)
80	0.895 (6.6)	0.864 (6.7)	0.802 (6.5)	0.647 (6.9)	0.517 (7.2)	0.343 (11.3)	0.233 (11.1)	0.157 (19.7)	0.101 (7.7)
85	—	0.810 (6.6)	—	—	0.439 (7.5)	0.284 (7.6)	0.202 (13.0)	0.148 (17.3)	0.080 (8.7)
90	0.838 (6.9)	0.742 (7.7)	0.642 (6.5)	0.496 (6.6)	0.373 (7.3)	0.278 (7.7)	0.186 (10.2)	0.138 (12.1)	0.070 (8.6)
95	—	0.696 (7.5)	—	—	0.345 (7.5)	0.274 (7.8)	0.183 (12.9)	0.137 (15.2)	0.066 (8.2)
100	0.805 (6.5)	0.622 (6.8)	0.534 (6.4)	0.409 (6.5)	0.333 (6.4)	0.305 (7.4)	0.197 (10.5)	0.136 (12.1)	0.068 (8.8)
105	—	0.625 (7.1)	—	—	0.355 (7.1)	0.326 (7.6)	0.213 (8.1)	0.166 (12.7)	0.082 (7.6)
110	0.774 (6.9)	0.597 (7.5)	0.472 (6.5)	0.395 (6.4)	0.366 (6.7)	0.382 (6.5)	0.246 (9.6)	0.206 (10.0)	0.110 (7.8)
115	—	0.568 (7.6)	—	—	0.404 (7.2)	0.436 (9.3)	0.294 (7.9)	0.262 (10.8)	0.152 (8.1)
120	0.761 (6.9)	0.538 (6.4)	0.443 (6.3)	0.421 (6.4)	0.448 (6.9)	0.472 (7.5)	0.326 (11.4)	0.315 (18.3)	0.206 (9.9)
125	—	0.526 (6.8)	—	—	0.473 (6.4)	0.511 (8.4)	0.382 (13.3)	0.417 (15.3)	0.277 (7.6)
130	0.750 (6.5)	0.517 (6.7)	0.441 (6.5)	0.470 (6.5)	0.519 (6.7)	0.536 (7.4)	0.454 (13.7)	0.498 (18.6)	0.345 (8.7)

transition and 25–27% for the $v = 0 \rightarrow 4$ transition, the actual value depending on the incident energy.

Table 4. Absolute rovibrational ($0 \rightarrow 1$) DCSs (10^{-18} cm^2 sr^{-1}) for electron scattering from nitric oxide. Figures in brackets indicate the absolute uncertainty expressed as a percentage.

	E_0 (eV)					
θ_e°	7.5	10.0	15.0	20.0	30.0	40.0
10	—	2.277 (15.3)	3.673 (16)	2.017 (16.5)	0.758 (17.0)	1.224 (18.7)
20	0.755 (17)	0.689 (15.3)	2.541 (16)	1.337 (16.5)	0.292 (17.0)	0.238 (18.7)
30	0.457 (17)	0.427 (15.3)	2.168 (16)	0.895 (16.5)	0.233 (17.0)	0.116 (18.7)
40	0.320 (17)	0.343 (15.3)	1.590 (16)	0.725 (16.5)	0.128 (17.0)	0.108 (18.7)
50	0.221 (17)	0.324 (15.3)	1.685 (16)	0.672 (16.5)	0.132 (17.0)	0.100 (18.7)
60	0.214 (17)	0.378 (15.3)	1.766 (16)	0.649 (16.5)	0.095 (17.0)	0.085 (18.7)
70	0.169 (17)	0.356 (15.3)	1.713 (16)	0.659 (16.5)	0.110 (17.0)	0.077 (18.7)
80	0.119 (17)	0.350 (15.3)	1.496 (16)	0.540 (16.5)	0.104 (17.0)	0.053 (18.7)
90	0.089 (17)	0.365 (15.3)	1.430 (16)	0.477 (16.5)	0.103 (17.0)	0.047 (18.7)

Table 5. Absolute rovibrational ($0 \rightarrow 2$) DCSs (10^{-18} cm^2 sr^{-1}) for electron scattering from nitric oxide. Figures in brackets indicate the absolute uncertainty expressed as a percentage.

	E_0 (eV)					
θ_e°	7.5	10.0	15.0	20.0	30.0	40.0
10	—	0.086 (16.5)	0.689 (18)	0.408 (18)	—	—
20	—	0.063 (16.5)	0.568 (18)	0.352 (18)	—	—
30	—	0.062 (16.5)	0.520 (18)	0.240 (18)	—	—
40	—	0.064 (16.5)	0.427 (18)	0.224 (18)	—	—
50	—	0.059 (16.5)	0.495 (18)	0.191 (18)	—	—
60	—	0.075 (16.5)	0.509 (18)	0.180 (18)	—	—
70	—	0.074 (16.5)	0.503 (18)	0.166 (18)	—	—
80	—	0.081 (16.5)	0.437 (18)	0.132 (18)	—	—
90	—	0 085 (16.5)	0.421 (18)	0.096 (18)	—	—

Table 6. Absolute rovibrational ($0 \rightarrow 3$) DCSs (10^{-18} cm^2 sr^{-1}) for electron scattering from nitric oxide. Figures in brackets indicate the absolute uncertainty expressed as a percentage.

	E_0 (eV)					
θ_e°	7.5	10.0	15.0	20.0	30.0	40.0
10	—	0.051 (20)	0.390 (21)	0.143 (23)	—	—
20	—	0.046 (20)	0.219 (21)	0.145 (23)	—	—
30	—	0.040 (20)	0.207 (21)	0.095 (23)	—	—
40	—	0.036 (20)	0.165 (21)	0.080 (23)	—	—
50	—	0.031 (20)	0.189 (21)	0.076 (23)	—	—
60	—	0.034 (20)	0.201 (21)	0.071 (23)	—	—
70	—	0.033 (20)	0.198 (21)	0.058 (23)	—	—
80	—	0.030 (20)	0.168 (21)	0.045 (23)	—	—
90	—	0.034 (20)	0.153 (21)	0.035 (23)	—	—

Table 7. Absolute rovibrational ($0 \rightarrow 4$) DCSS (10^{-18} cm^2 sr^{-1}) for electron scattering from nitric oxide. Figures in brackets indicate the absolute uncertainty expressed as a percentage.

	E_0 (eV)					
θ_e°	7.5	10.0	15.0	20.0	30.0	40.0
10	—	—	0.154 (25)	0.067 (27)	—	—
20	—	—	0.107 (25)	0.068 (27)	—	—
30	—	—	0.084 (25)	0.052 (27)	—	—
40	—	—	0.080 (25)	0.036 (27)	—	—
50	—	—	0.085 (25)	0.029 (27)	—	—
60	—	—	0.090 (25)	0.028 (27)	—	—
70	—	—	0.089 (25)	0.025 (27)	—	—
80	—	—	0.072 (25)	0.018 (27)	—	—
90	—	—	0.065 (25)	0.017 (27)	—	—

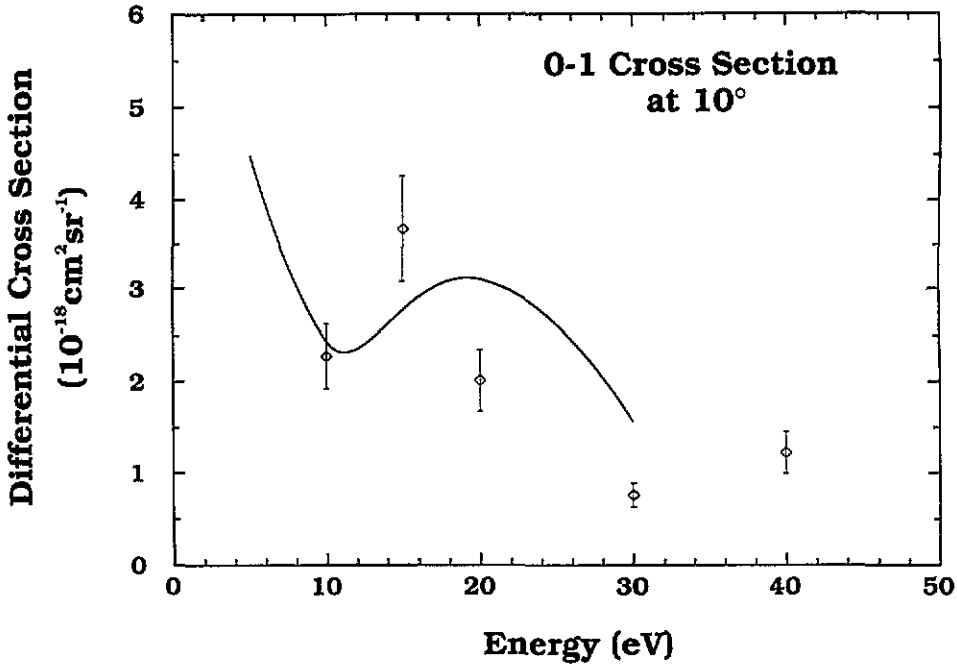

Figure 5. Energy dependence of the $v = 0 \rightarrow 1$ DCS, in units of 10^{-18} cm^2 sr^{-1}, at $\theta_e = 10°$. The present data (◇) are compared against the BCSVM calculation of Mu-Tao Lee (——).

An interesting and quite informative way of viewing the present data is given in figure 5, where we look at the energy dependence of the $v = 0 \rightarrow 1$ transition at $\theta_e = 10°$. Two points are immediately apparent from this figure. First there is a broad structure in the experimental rovibrational cross section, centred at about $E_0 = 15$ eV and second, that the theory, whilst also observing a broad structure, does not predict the same energy at which the peak in this cross section occurs. Evidence for the existence of resonance phenomena in the 12–20 eV energy range has been provided by Sanche and Schulz (1972). In their transmission spectra, they identified several structures associated with both core-excited Feshbach resonances and core-excited shape resonances. In the former case they identified

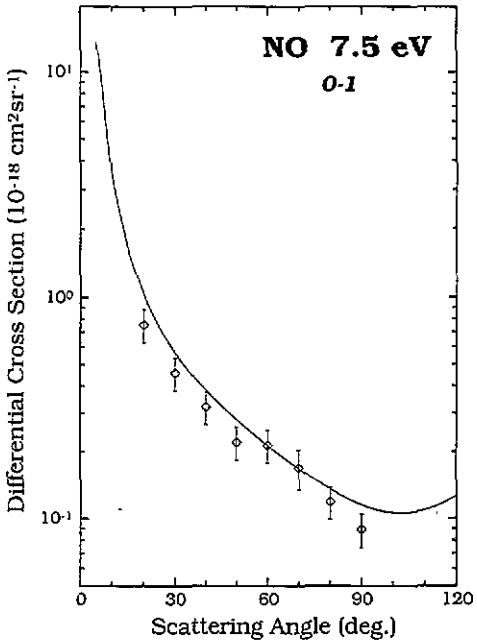

Figure 6. Differential cross sections, in units of 10^{-18} cm^2 sr^{-1}, for the $v = 0 \rightarrow 1$ rovibrational excitation in NO at 7.5 eV. The present data (◊) are compared against the BCSVM calculation of Mu-Tao Lee (——).

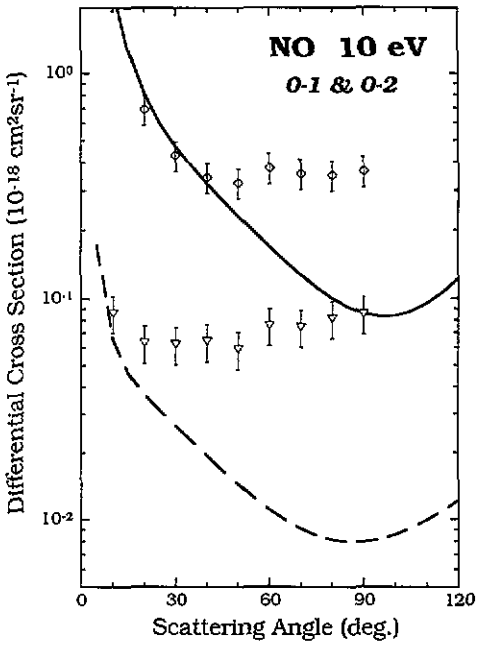

Figure 7. Differential cross sections, in units of 10^{-18} cm^2 sr^{-1}, for the $v = 0 \rightarrow 1$ and $v = 0 \rightarrow 2$ rovibrational excitation in NO at 10 eV. The present 0–1 (◊) and 0–2 (▽) data are compared against the corresponding BCSVM calculations of Mu-Tao Lee (——) and (– – –).

resonances associated with the grandparent $b^3\Pi$, $A^1\Pi$ and $B^1\Pi$ excited states of NO^+. These states were originally considered as likely candidates for compound-state formation from the ground molecular state on the basis that their internuclear separations were similar to that of the NO ground state (Edqvist *et al* 1970). In the latter case the core-excited shape resonances arise when singly or doubly excited states of the neutral molecule bind an extra electron by the centrifugal barrier. Furthermore, in their total cross section experiment, Szmytkowski and Maciag (1991) also found a broad structureless maximum centred around 16 eV. Consequently, we believe the structure of figure 5 to be associated with either one or more of the possible core-excited Feshbach resonances, or shape resonances of the NO negative ion in the 12–20 eV energy range. Note that the structure in figure 5 was also observed at all other angles for the $v = 0 \rightarrow 1$ transition and, similarly for the $v = 0 \rightarrow 2$ transition, although in this case the experimental cross section is always larger than that predicted by the theory, indicating that the theory is not accurately reproducing the correct branching ratio for these processes. Middleton *et al* (1994) recently noted in their studies of the $a^1\Delta_g$ and $b^1\Sigma_g^+$ electronic states of O_2 that the theoretically predicted position of a similar resonance peak, as calculated theoretically, was brought into better agreement with the experimental value when more channels were included in the calculation. Thus the lack of agreement here between the calculation of Mu-Tao Lee (1994) and the present experiment in the position of the observed structure (figure 5) may well be due to the calculation not including a sufficient number of channels. This result has important ramifications for the level of agreement between theory and experiment for the angular dependence of the DCSs,

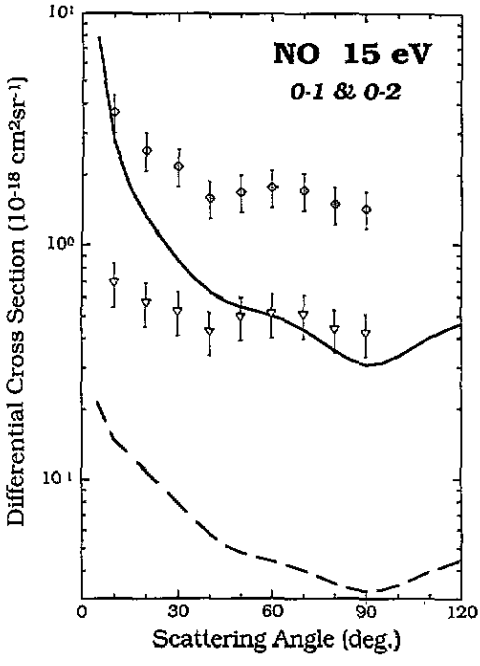

Figure 8. Differential cross sections, in units of 10^{-18} cm^2 sr^{-1}, for the $v = 0 \rightarrow 1$ and $v = 0 \rightarrow 2$ rovibrational excitation in NO at 15 eV. The present 0–1 (◇) and 0–2 (▽) data are compared against the corresponding BCSVM calculations of Mu-Tao Lee (——) and (– – –).

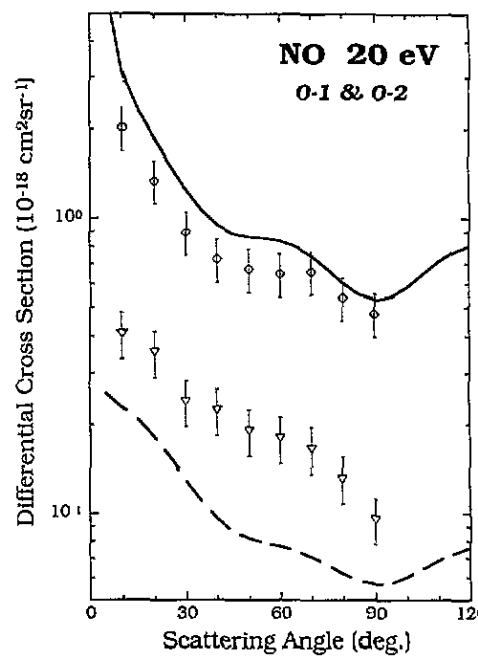

Figure 9. Differential cross sections, in units of 10^{-18} cm^2 sr^{-1}, for the $v = 0 \rightarrow 1$ and $v = 0 \rightarrow 2$ rovibrational excitation in NO at 20 eV. The present 0–1 (◇) and 0–2 (▽) data are compared against the corresponding BCSVM calculations of Mu-Tao Lee (——) and (– – –).

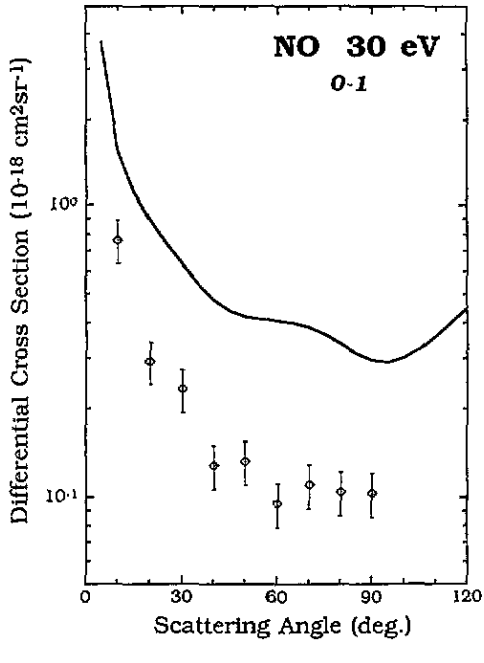

Figure 10. Differential cross sections, in units of 10^{-18} cm^2 sr^{-1}, for the $v = 0 \rightarrow 1$ rovibrational excitation in NO at 30 eV. The present data (◇) are compared against the BCSVM calculation of Mu-Tao Lee *et al* (——).

as we now discuss below.

The present 0–1 rovibrational DCS at 7.5 eV is given in figure 6 along with the result of the recent BCSVM calculation of Mu-Tao Lee. The level of agreement, in terms of both magnitude and shape, between theory and experiment is fair across the entire common angular range, the theory in general slightly overestimating the strength of the 0–1 excitation process. The data also indicate the possible existence of a shallow structure in the range $40° \leqslant \theta_e \leqslant 70°$, which the theory fails to predict.

In figure 7 we illustrate the current 0–1 and 0–2 rovibrational DCSs, as measured at 10 eV beam energy. In both cases we compare the present data with the relevant results of the BCVSM calculation of Mu-Tao Lee. For the $0 \rightarrow 1$ cross section the data are in very good agreement with theory for $\theta_e \leqslant 50°$ but thereafter the theory somewhat underestimates the strength of the cross section. On the other hand the level of agreement between theory and experiment for the 0–2 excitation is generally poor for all θ_e. The theory again underestimates the size of the cross section and, in this case, does not reproduce the shape of the experimental DCS which is essentially isotropic. At 15 eV the theory underestimates the magnitude of both the 0–1 and 0–2 DCSs (figure 8) across the measured angular range, although agreement in terms of shape is fair. This can be understood by the observation that the experiment finds the maximum resonance enhancement effect of both the 0–1 and 0–2 cross sections to be at about 15 eV whilst the theory predicts it to occur at a somewhat higher energy ($\sim$ 20 eV). Consequently, it is not surprising to find that at 20 eV the theory somewhat overestimates the magnitude of the 0–1 DCS. In this case, however, we would still characterize the overall level of agreement between theory and experiment as being fair, in particular the shape of the angular distribution for both the calculation and experiment are seen to be in good accord (figure 9) for the 0–1 transition at 20 eV. For the 0–2 transition at 20 eV (figure 9) there is also a fair level of agreement between theory and experiment for the shape of the angular distribution, although the theory seriously underestimates the magnitude of the DCS. This is consistent with what we saw previously at both 10 and 15 eV and establishes the clear trend that the calculation does not reproduce the correct branching ratio between the 0–2 transition to the 0–1 transition, at the energies we have studied. In figure 10, the 30 eV 0–1 DCS is again plotted with the result of the calculation of Mu-Tao Lee. In this case the theory significantly overestimates the magnitude of the cross section although, as before, the shapes of the experimental and theoretical angular distributions are in quite good accord. As there was no theory available for comparison with our 40 eV 0–1 DCS, we do not plot it or discuss it further here except to note that, like the data at 15, 20 and 30 eV, it is strongly peaked in the forward direction, reflecting the effect of the permanent dipole moment of the NO molecule.

The present experimental DCSs for the 0–1 and 0–2 transitions are all extrapolated to 0° and 180° using the theory of Mu-Tao Lee as a guide (see the preceding section for a broader discussion of this point) and then integrated to generate total rovibrational cross sections. Due to the quite large uncertainties associated with extrapolating the present data from 100–180°, the errors on the 0–1 and 0–2 integral cross sections varied from 25 to 35%. Note that whilst we do not plot these data the integral cross sections can be found in table 1. Also found in table 1 is our current estimate of the 'grand' total cross section for NO. In the present case this is defined as

$$Q_{\mathrm{TOT}}(E_0) = \sum_{i=0}^{2} Q_i(E_0) = Q_{\mathrm{el}}(E_0) + Q(E_0)_{0-1} + Q(E_0)_{0-2}.$$

Clearly, our derived values represent lower bounds on the true value of the total cross section for NO as there are, in general, other open rovibrational and electronic-state channels, and

ionization processes to be considered. Using the ionization cross sections of Rapp and Englander-Golden (1965) and adding these to our values of $Q_{TOT}(E_0)$ from table 1, we arrive at figure 11 where the modified estimates of our present grand total cross section are plotted along with the values from the experiment of Szmytkowski and Maciag (1991). As expected the current values for the grand total cross section are still smaller than those of Szmytkowski and Maciag (1991) with the level of agreement improving as we go to lower values of E_0, where there are fewer unaccounted open channels.

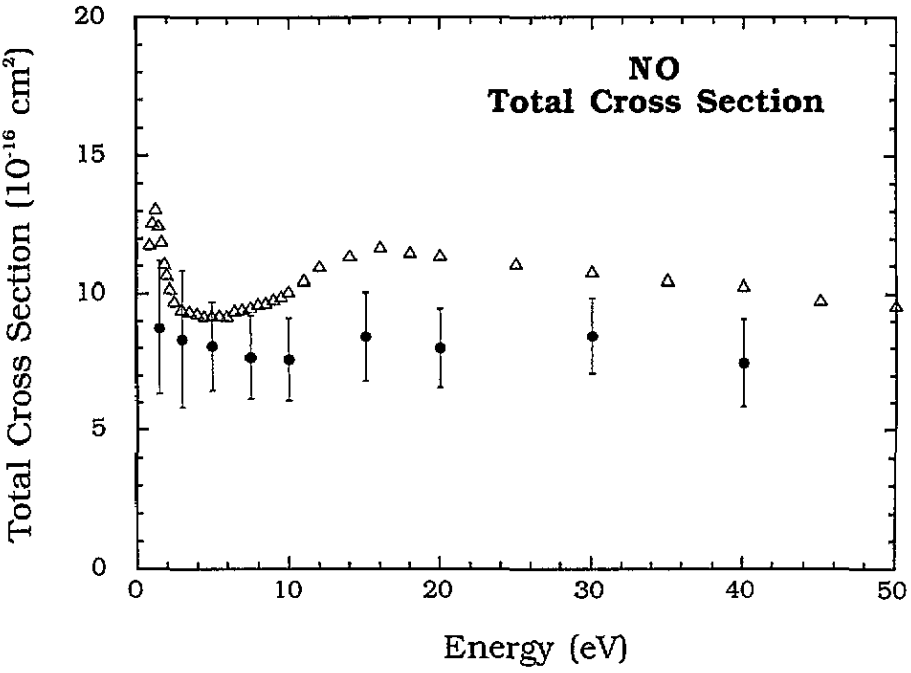

Figure 11. Grand total cross section, in units of 10^{-16} cm^2, for electron scattering from NO. The present estimates (●) are compared against the data of Szmytkowski and Maciag (△).

4. Conclusions

We have reported absolute DCSs for elastic scattering and rovibrational excitation of electrons from NO. The present elastic data have extended the earlier measurements of Kubo *et al* (1981) and significantly reduced the error limits on the cross sections. Comparison of the current elastic data with the BCSVM calculation of Mu-Tao Lee *et al* (1992) found that whilst the theory, in general, reproduced the gross features of the DCSs it quite often failed in calculating the detailed structure. Our absolute rovibrational DCSs are the first to be reported in the literature. Comparison of these data with the recent calculation by Mu-Tao Lee (1994) found only marginal agreement, the calculation often reproducing the shape of the DCSs but failing to predict their magnitudes correctly. Clearly, at this time, the BCSVM technique appears to be superior in calculating DCSs for elastic scattering over those for the rovibrational channels.

Acknowledgments

The Flinders experiments were supported in part by a grant from the Australian Research Council (ARC). MJB also acknowledges the ARC for additional financial support through a Postdoctoral Fellowship. We gratefully acknowledge the collaborative grants scheme of the ANU which has facilitated this work. RJG thanks the ANU for a postgraduate scholarship, AGM thanks Flinders University for a postgraduate scholarship and BM thanks the Australian Government for his APRA. We thank Dr Mu-Tao Lee for providing us with tables of his data, some of which was prior to its publication.

References

Boness M J W and Hasted J B 1966 *Phys. Lett.* **21** 526–8
Boness M J W, Hasted J B and Larkin I W 1968 *Proc. R. Soc.* A **305** 493–515
Brion C E, Cook J P D, Fuss I and Weigold E 1982 *Chem. Phys.* **64** 287–97
Brüche E 1927 *Ann. Phys., Lpz.* **83** 1065–128
Brunger M J and Teubner P J O 1990 *Phys. Rev.* A **41** 1413–26
Buckman S J, Gulley R J, Moghbelalhossein M and Bennett S J 1993 *Meas. Sci. Technol.* **4** 1143
Burrow PD 1974 *Chem. Phys. Lett.* **26** 265–8
Camilloni R, Fainelli E, Petrocelli G and Stefani G 1987 *J. Phys. B: At Mol. Phys.* **20** 1839–51
Clautier G G and Schiff H I 1959 *J. Chem. Phys.* **31** 793–9
Dalba G, Fornasini P, Grisenti R, Ranieri G and Zecca A 1980 *J. Phys. B: At. Mol. Phys.* **13** 4695–701
da Paixao F J, Lima M A P and McKoy V 1993 *Proc. 18th Int. Conf. on Physics of Electronic and Atomic Collisions (Aarhus)* Abstracts p 333
Dorman F H 1966 *J. Chem. Phys.* **44** 3856–63
Edqvist O, Lindholm E, Selin L E, Sjörgren H and Asbrink L 1970 *Ark. Fys.* **40** 439
Ehrhardt H and Willmann K 1967 *Z. Phys.* **204** 462–73
Fantoni R, Giardini-Guidoni A and Tiribelli R 1982 *J. Elect. Spectrosc. Relat. Phenom.* **26** 99–105
Frost D C and McDowell C A 1958 *J. Chem. Phys.* **29** 1424–5
Gianturco F A and Jain A 1986 *Phys. Rep.* **143** 347
Gresteau F, Hall R I, Huetz A, Vichon D and Mazeau J 1979a *J. Phys. B: At. Mol. Phys.* **12** 2925–35
—— 1979b *J. Phys. B: At. Mol. Phys.* **12** 2937–45
Gresteau F, Hall R I, Mazeau J and Vichon D 1977 *J. Phys. B: At. Mol. Phys.* **10** L545–8
Gulley R J, Alle D T, Brennan M J, Brunger M J and Buckman S J 1994 *J. Phys. B: At. Mol. Opt. Phys.* **27** 2593–611
Hagstrum H D and Tate J T 1941 *Phys. Rev.* **59** 354–70
Hasted J B and Awan A M 1969 *J. Phys. B: At. Mol. Phys.* **2** 367–80
Hierl P M and Franklin J L 1967 *J. Chem. Phys.* **47** 3154–61
Imami M and Borst W L 1975 *J. Chem. Phys.* **63** 3602–5
Jain A K, Kumar P and Tripathi A N 1993 *Proc. 18th Int. Conf. on Physics of Electronic and Atomic Collisions (Aarhus)* Abstracts p 251
Kadota K and Kaneko Y 1977 *J. Phys. Soc. Japan* **42** 250–4
King G C, McConkey J W, Read F J and Dobson B 1980 *J. Phys. B: At. Mol. Phys.* **13** 4315–23
Kirby K P 1993 *The Physics of Electronic and Atomic Collisions* (New York: AIP) pp 48–58
Koike F 1975 *J. Phys. Soc. Japan* **39** 1590–5
Krishnakumar E and Srivastava S K 1988 *J. Phys. B: At. Mol. Opt. Phys.* **21** L607–9
Kubo M, Matsunaga D, Koshio K, Suzuki T and Tanaka H 1981 *At. Coll. Res. Japan* **7** 4–5
Mu-Tao Lee 1994 Private communication
Mu-Tao Lee, Fujimoto M M, Michelin S E, Machado L E and Brescansin L M 1992 *J. Phys. B: At. Mol. Opt. Phys.* **25** L505–10
Mason N J and Newell W R 1989 *J. Phys. B: At. Mol. Opt. Phys.* **22** 2297–309
Mazeau J, Gresteau F, Hall R I and Huetz A 1978 *J. Phys. B: At. Mol. Phys.* **11** L557–60
Middleton A G, Brunger M J, Teubner P J O, Anderson M W B, Noble C J, Woeste G, Blum K, Burke P G and Fullerton C 1994 *J. Phys. B: At. Mol. Opt. Phys.* **27** 4057
Nesbet R K 1979 *Phys. Rev.* A **20** 58

Nickel J C, Zetner P W, Shen G and Trajmar S 1989 *J. Phys. E: Sci. Instrum.* **22** 730–8
Norcross D W and Collins L A 1982 *Advances in Atomic and Molecular Physics* vol 18 (New York: Academic) p 341
Povch M M, Skubenich V V and Zapesochnyi I P 1972 *Opt. Spektrosc.* **32** 1044–5
Rapp D and Briglia D D 1965 *J. Chem. Phys.* **43** 1480–9
Rapp D and Englander-Golden D 1965 *J. Chem. Phys.* **43** 1464–79
Register D F, Trajmar S and Srivastava S K 1980 *Phys. Rev.* A **21** 1134–51
Rohr K 1977 *J. Phys. B: At. Mol. Phys.* **10** 2215
Sanche L and Schulz G J 1972 *Phys. Rev.* A **6** 69–86
Skubenich V V, Povch M M and Zapesochnyi I P 1977 *High Energy Chemistry (Russian origin)* **11** 92–5
Spence D and Schulz G J 1971 *Phys. Rev.* **3** 1968–76
Srivastava S K, Chutjian A and Trajmar S 1975 *J. Chem. Phys.* **63** 2659–65
Stone E J and Zipf E C 1972 *J. Chem. Phys.* **56** 2870–4
Sullivan J P, Gibson J, Gulley R J and Buckman S J 1994 Private communication
Sun W, Morrison M A, Isaacs W A, Alle D T, Gulley R J, Brennan M J and Buckman S J 1994 *J. Phys. B: At. Mol. Opt. Phys.* in preparation
Szmytkowski C and Maciag K 1991 *J. Phys. B: At. Mol. Opt. Phys.* **24** 4273–9
Tanaka H, Srivastava S K and Chutjian A 1978 *J. Chem. Phys.* **69** 5329
Teillet-Billy D and Fiquet-Fayard F 1977 *J. Phys. B: At. Mol. Phys.* **10** L111–17
Tennyson J and Noble C J 1986 *J. Phys. B: At. Mol. Phys.* **19** 4025–33
Tronc M, Huetz A, Landau M, Pichou F and Reinhardt J 1975 *J. Phys. B: At. Mol. Phys.* **8** 1160–9
Tronc M, King G C and Read F H 1980 *J. Phys. B: At. Mol. Phys.* **13** 999–1008
van Brunt R J and Kieffer L J 1974 *Phys. Rev.* A **10** 1633–7
van Sprang H A, Brongersma H H and de Heer F J 1979 *Chem. Phys. Lett.* **65** 55
Zecca A, Lazzizzera I, Krauss M and Kuyatt C E 1974 *J. Chem. Phys.* **61** 4560–6